Journal of Neonatal Surgery
ISSN(Online): 2226-0439
Vol. 14, Issue 11s (2025)
https://www.jneonatalsurg.com

OPEN ACCESS

Enhancing Detection and Classification of Neurological Cancer Images using An Artificial Neural Network

D Jareena Begum[1], M. Diviya[2]

[1,2]Research Scholar, Department of Computer Science and Engineering, Amrita School of Computing, Chennai, Amrita Vishwa Vidyapeetham, India.

D JareenaBegum, Email ID: dj_begum@ch.students.amrita.edu

M.Diviya, Email ID: diviyalouis@gmail.com

Cite this paper as: D Jareena Begum, M. Diviya, (2025) Enhancing Detection and Classification of Neurological Cancer Images using An Artificial Neural Network. *Journal of Neonatal Surgery*, 14 (11s), 391-402.

ABSTRACT

Early cancer diagnosis using inexpensive and fast techniques could save many lives. Late-stage cancer treatment is difficult. Invasive or non-invasive brain cancer diagnosis is possible. ANN architecture must be carefully chosen for the application, as biopsy is intrusive. This research proposes a functional ANN model to improve diagnosis procedures. ANN research is hot in radiology, cardiology, and oncology. This study used ANNs in medicine. The study also attempted brain tumor diagnosis application. The MR picture requires the neural network to assess brain health. In the hands of human clinicians, this process has a high computational complexity. Experienced radiologists are necessary for accurate classification and segmentation of the brain tumour. We suggest a computer-aided diagnosis-based strategy for segmenting brain tumours as a means of getting around these problems. Below are the steps that make up the proposed artificial neural network and random forest algorithm, support vector machine method. An asymmetrical gradient filter is applied during preprocessing to reduce background noise and even out intensity variations. The artificial neural network is then used to determine if the input brain image is normal or pathological. The result is a model in the vector space. A greater success rate of 2.31% is achieved using the proposed strategy. When compared to other techniques, this one has a sensitivity of 5.81% and a specificity of 2.28%, respectively.

Keywords: *Artificial neural network, Brain tumour, human clinicians, Pathologist, Curvelet transform*

1. INTRODUCTION

The WHO estimates 251,329 brain tumour deaths per year. The National Brain Tumour Foundation (NBTF) [1] reports that brain tumour deaths in low- and middle-income nations have tripled. Brain tumours can affect toddlers and adults. 85%–90% of the primary Central Nervous System (CNS) malignancies are brain tumours. Brain tumours affect 11,700 people annually. For patients with a malignant brain or CNS tumour, the 5-year survival rate is approximately 34% for men and 36% for women. Brain tumours are benign, malignant, pituitary, or other. Proper therapy, planning, and diagnosis extend patient lives. MRI detects brain tumours best [2]. Brain tumours must be detected and diagnosed quickly. Computer science's artificial intelligence (AI) researches human-like hardware and software. AI-enhanced programmes can learn, plan, and solve problems. AI has many benefits [41–45]. These include helping professionals with challenging operations, decision-making, and jobs, giving accurate Brain Tumour in images, minimising composite handling risks, boosting Brain Tumour information about individual behaviour, and more.

Brain cancer kills most Asians [1]. Brain or spinal cord cancer [2]. Brain tumours are categorised by origin, growth rate, and progression [3,4]. Malignant or benign brain tumours. Meningiomas, pituitary tumours, and astrocytomas (WHO Grade-I) are benign brain tumours that seldom invade healthy cells, have defined borders, and grow slowly.

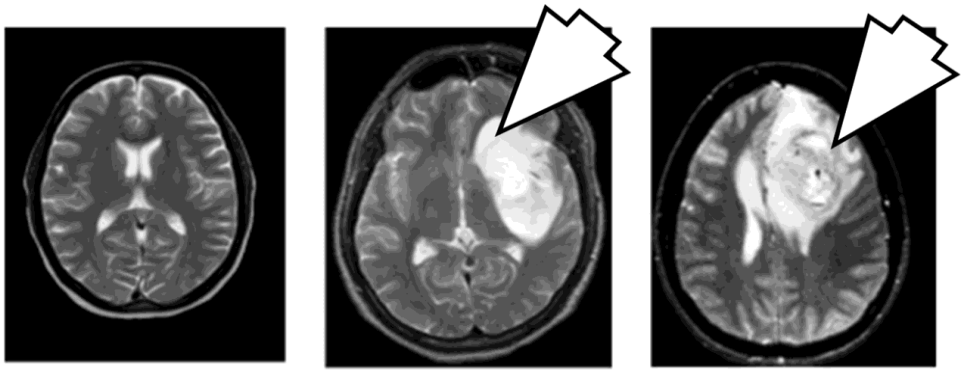

(a) (b) (c)

Brain tumours can be primary or secondary. Brain tumours originate. Secondary brain tumours or metastases occur when cancer in another organ spreads to the brain. Brain tumours are classed by malignant cell proliferation from low to high. The WHO divides brain tumours into four growth rates [2,5-9] (see below). Brain tumours are also staged (0, 1, 2, 3, and 4). Stage-0 cancer cells are abnormal but do not spread. Stages 1–3 indicate fast-growing cancer cells. Finally, Stage 4 cancer spreads throughout the body. Early cancer diagnosis using inexpensive and fast techniques could save many lives. Late-stage cancer treatment is difficult. Invasive or non-invasive brain cancer diagnosis is possible. To analyse a cancer sample, biopsy requires a skin incision. Pathologists examine tumour cells under a microscope to confirm cancer. Body and brain imaging are non-invasive methods. CT and MRI are faster and safer than biopsy. These imaging tools help radiologists diagnose brain illnesses, track disease progression, and plan surgery [10].

Early cancer diagnosis using inexpensive and fast techniques could save many lives. Late-stage cancer treatment is difficult. Invasive or non-invasive brain cancer diagnosis is possible. ANN architecture must be carefully chosen for the application, as biopsy is intrusive. Choosing an application-appropriate network type, b. Layer count. Hidden layer nodes and d. Interlayer functions. Network generalisation is how well a neural network handles different data kinds. Despite well-designed and trained ANN that decreases performance error to the minimum amount, ANN fails when given fresh input data and performs poorly. Artificial neural networks have been used in brain cancer detection studies. Kumar and Raju (2) use textural features and neuro classification logic to predict brain cancer early using computer-aided diagnostics. Cluster microclassification and tumour mass detection predicted malignancy. Nine invariant traits and the cancer prediction minimal distance were used to predict tumours in MRI images. Kadam et al. (3) suggested a hardware-and-software neural network brain cancer detection system. To simplify processing and analysis, an adaptive filter removed spurious signals and scaled the image. Segmented the ROI. Haralick's grey tone spatial dependence matrix was used to obtain eight texture features from cancer and normal regions. Back propagation neural networks were trained to detect brain cancers (2). Brain Tumour A "tumour," which meaning "swelling," is any condition that causes a lump or mass in the body. Neoplasms, or malignancies, are characterised by tumours. Infections and other disorders can generate tumours, making imaging diagnosis challenging (4). Neoplasms arise from normal body cells that no longer respond to growth-limiting physiological processes. Uncontrolled growth causes tumours. Malignant tumours grow rapidly, invade adjacent tissues, and metastasis (5). Even a minor brain tumour might cause problems. Primary and secondary brain tumours differ in genesis. a. Brain tumours are primary. b. Lung and breast cancers start elsewhere and travel to the brain. Primary brain tumours cannot be removed. Brain tumours can be classified by cell type and microscopic appearance. Oligodendroglioma, meningioma, and glioblastoma are common (6). Scanners identify, classify, stage, and compare cancers. Based on suspicion, detection can be diagnosed, case found, or screened. Cancer referrals (1). MR imaging locates tumours, however visual inspection alone cannot identify their types. ANN can improve diagnosis by identifying all pixel correlations and variations. The brain controls other organs and helps make decisions [10].

1.1 Contribution

In this section, our contribution in this research paper has been presented. The aforementioned previous approaches have drawbacks such as low segmentation accuracy, poor tumor segmentation findings, low immunity to noise and artefacts, and low sensitivity and specificity. To address this issue, we offer a novel method for classifying and segmenting the tumour in MR brain images using an anisotropic diffusion filtered support vector machine RF approach. The MR brain image is then sent into a neural network support vector machine RFclassifier. Anisotropic filters typically perform preprocessing on an image in order to improve it and get rid of any artefacts that could have been present to begin with. After the image has been preprocessed, features are obtained using the ANN-SVM-RF classifier, and the picture is then labelled as having either high (abnormal) or low (normal) brain volume. Next, the high-density MR brain picture undergoes a morphological procedure to segment the tumour area. This article's structure can be summarized as follows: The Literature Survey is presented in Section

2. The artificial neural network and random forest algorithm, support vector machine classifier presented here are discussed in detail in Sections 3 and 4, respectively. The paper's findings and comments are presented in Section 5, and it concludes in Section 6.

2. RELATED WORKS

The word bio The Convolutional Neural Network (CNN) was utilised to diagnose meningioma, glioma, and pituitary cancers with 91.3% accuracy and recall of 88%, 81%, and 99%, respectively. MRI slices were utilised to classify brain cancers using 2D convolutional neural networks. This article uses data collection, preprocessing, modelling, optimisation, and hyper parameter adjustment. To assess model generalizability, the full dataset was cross validated 10-fold.

[1] The brain directs and coordinates body functions. It controls the central nervous system's daily voluntary and involuntary processes. Our brain's fibrous tumour grows unchecked. Radiologists use magnetic resonance imaging (MRI) to prevent and treat brain cancers. This study found brain tumours. Much research has been done in the following fields: The main purpose of [1] was to demonstrate the produced findings, which were an average of 0.82 dice similarity index, which was better because it showed better overlap between the extracted tumour region and the manually extracted tumour by radiologists. The author tested ResNet, DenseNet, and Mobile Net in [2,] and found accuracy of 91.8, 92.8, and 92.9.

In [3,] picture segmentation was done using TK means clustering to find the cancer. In [4], different ensemble approaches like KNN-RF-DT are used to compute the region of the tumer and construct a suitable voting mechanism. 2556 photos yielded 97.3% accuracy.

According to Tandel et al. Five clinical multiclass datasets were produced by him. Brain tumour categorization was enhanced using MRI images and a Convolutional Neural Network (CCN) trained with transfer learning. Several other classification strategies were tested against CNN, including Decision Trees, Naive Bayeses, Linear Discrimination, K-Nearest Neighbors, and Support Vector Machines (SVM). On five different multiclass classification brain tumour datasets, the CNN-based (DL) model achieved better results than six machine learning model techniques. After being subjected to K2, K5, and K10 cross-validation, the CNN-based AlexNet achieved mean accuracy values of 87.14, 93.74, 95.97, 96.65, and 100% across five classes, respectively.

KNN, SVM, DT, NB, EM, RF, and others are the most common ML methods for medical image analysis. Researchers used many of them to analyse brain images. Table 4 lists some. ML-based brain cancer categorization methods follow. Texture, brightness, and contrast are used to create mathematical models for feature extraction. ML algorithms sometimes combine variables from many extraction models to better discrimination [17]. K-Nearest Neighbours (KNN) [18] and Support Vector Machines (SVM) [19] are two popular brain image categorization and segmentation methods.

3. PROPOSED ALGORITHM

3.1 Feature extraction using Curvelet transform

The Multi-scale analysis was not possible with the ridgelet transform, but it is with the curvelet transform. Therefore, we kick things off with a definition of a ridgelet transform [19].

As an example (1), we can express the ridgelet coefficients for a given image as a series of numbers:

$$f(c,t,\theta) = \int\int \psi_{c,t,\theta}(x,y) f(x,y) dxdy \qquad (1)$$

Scale factor an, rotation angle, translation t, rotation R, and angle between zero and two. The term "ridgelet" will be used in the following two sentences:

$$\psi_{c,t,\theta}(x,y) = c^{-\frac{1}{2}\psi}\left(\frac{x\cos\theta + y\sin\theta tb}{c}\right) \qquad (2)$$

The sign denotes the ridgelet orientation, and the ridgelets maintain a constant profile along the lines. Unlike the ridgelet transformation, the curvelet transformation is able to tightly capture edge information across all scales. Combining the benefits of the Radon and wavelet transforms, the ridgelet-based curvelet transform is a powerful tool.

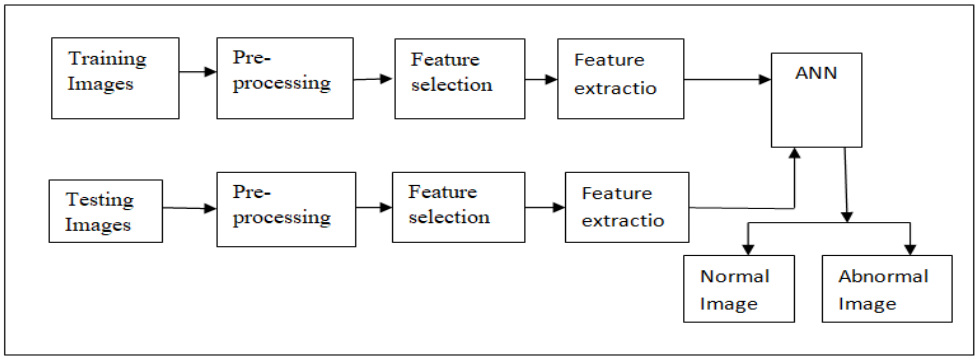

Fig. 2 Proposed brain tumor detection block diagram

The curvelet method divides the input picture into several bands. Each of these is partitioned into multiple blocks for ridgelet analysis. The Radon transform, a 1-dimensional wavelet transform, is utilised to realise the ridgelet transform. To lessen the impact of obstructions, ridgelets alter space with overlapping panes. A great deal of effort is wasted as a result of this. However, this process is extremely sluggish, making it unsuitable for data analysis in large datasets.

3.2 Radom Forest classifier

The suggested method employs binary classification via the RF algorithm. During the training phase, RF builds a large number of decision trees and produces a class with an average forecast. Using a grid search, the RF hyper-parameters were fine-tuned. Table 9 displays the variety of parameter settings used in grid search. Training a random forest with the optimal set of parameters recovered from the grid search yielded the highest possible classification accuracy. We use a confidence of 0.5 in the voting method and the Gini impurity criterion (split criterion) to determine the optimal number of random trees to generate; we prune and pre-prune; the minimum leaf size is 2; and the minimum size for splitting is 4. The Gini coefficient is based on:

$$(G)^n = \sum_{kj=1}^{nC} \binom{Pn}{kj} 1 - pj^k pj^{nC-kj}$$

where C is the total number of categories and p(j) is the chance of picking instance j.

For each attribute, we first determine its T2 metric by analysing its conditional mean and variance under the 'Num = 1' and 'Num = 0' conditions, respectively.

$$(RFT)^2 = [X1 - X0] + \left(\frac{mnx}{1!} + \frac{mn(n-1)SP^2}{2!}\right)$$

where X1 is the mean when Num = 1 and X0 is the mean when Num = 0 and Sp is defined as follows:

$$SP^n = \left(1 + \frac{mnx - 1}{n0 + 1!} + \frac{mn(n-1)S1^2}{n1 + n0 + 2!}\right)$$

where n1 is the sample size when Num = 1, and n0 is the sample size when Num = 0. Furthermore, the standard deviations for Num = 1 and Num = 0 are S1 and S0, respectively. When Num = 1 and 0 the statistical analysis is performed on all the attributes in the specified datasets. Additionally, the T2 metric is determined in data sets.

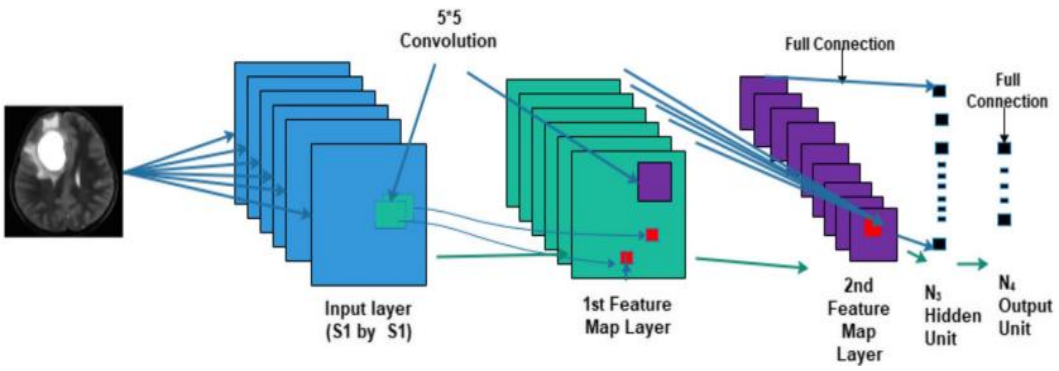

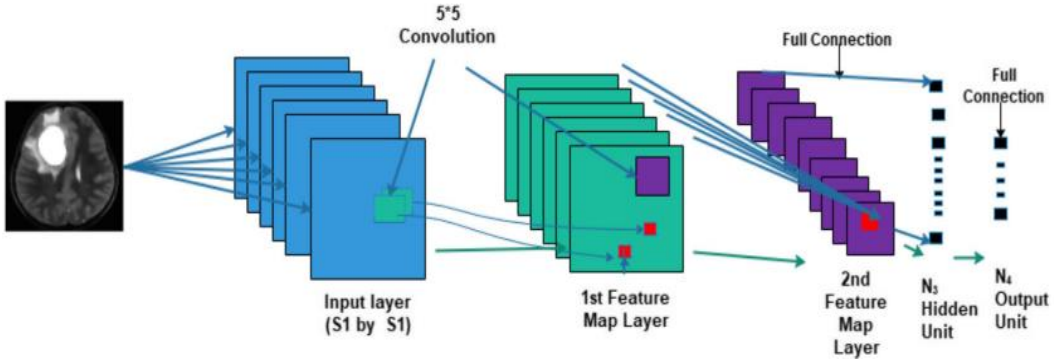

Fig. 3 Proposed brain tumor detection architecture ANN-RF-SVM layer diagram

When compared to other popular machine learning methods, random forest classifier (RF) performs exceptionally well in both classification and regression. And training and setting user-defined parameters is a breeze. Fig. 7 depicts the structure of the random forest model that we employ in our work to categorise the grip rectangle. The number (8) stands for the input dataset we used.

RFT = {(rf1, rf1), (rf2, rf2), ..., (rN , fN)} (8)

where ri is a vector of input features and fi is a bool value (-1 for poor grasp and 1 for good grasp). Instances of grip number N. Additionally, the dimension of our input feature ri, M, is equal to wf hf 7 = 4032. Instructions for training a random forest classifier are outlined below. First, select n training examples from these N occurrences randomly while replacing some of them. Next, choose m characteristics (mxn).

The grayscale morphological procedure is employed in this suggested effort to isolate MR brain tumours. The threshold is computed using the opening and closing Grayscale morphological processes. Smoothing out the MRI image's contour parts with a closure operation. The contour parts have gaps and holes that are closed during the closure operation. Given a structural element E, closure procedure Brain tumours are excellent examples of abnormal binary images.

4. ARTIFICIAL NEURAL NETWORK RANDOM FOREST CLASSIFIER

Artificial Neural Networks mirror human brains. Like neurons in our nervous system, the ANN can learn from input and predict or classify. Nonlinear statistical models like ANNs use complicated input-output interactions to find new patterns. These neural networks do image recognition, speech recognition, machine translation, and medical diagnosis. ANN benefits by learning from examples. ANN is mostly used for random function approximation. These technologies enable cost-effective distribution specification. ANN can also generate output from sample data. ANNs improve data analysis due to their high prediction abilities. Artificial Neural Network Architecture resembles neurons in our nervous system. Warren S. McCulloch and Walter Pitts coined "Neural Networks" in the early 1970s. ANNs must be structured to be understood. Neural networks require three layers. Input Layers An ANN's input layer receives text, numbers, audio files, image pixels, etc. Hidden layers are crucial to the ANN model. A perceptron has one or more hidden layers. These hidden layers recognise patterns in input data via mathematical calculations. The output layer receives the middle layer's rigorous computations. Many neural network characteristics and hyper parameters affect model performance. These parameters most affect ANN output. Weights, biases, learning rate, batch size, etc. ANN nodes have weights. Network nodes have weights. For calculating the weighted input total and bias.

Applying ANN to the brain tumour dataset involves these steps:

- Import necessary packages.
- Data directory import.
- Label and store the photos in the Data Frame.
- Reading each shot changes the image size to 256x256.
- Image normalisation
- Train, validate, and test the dataset.
- Model it.
- Model it.
- Train set and model.

- Test the model on the test set.

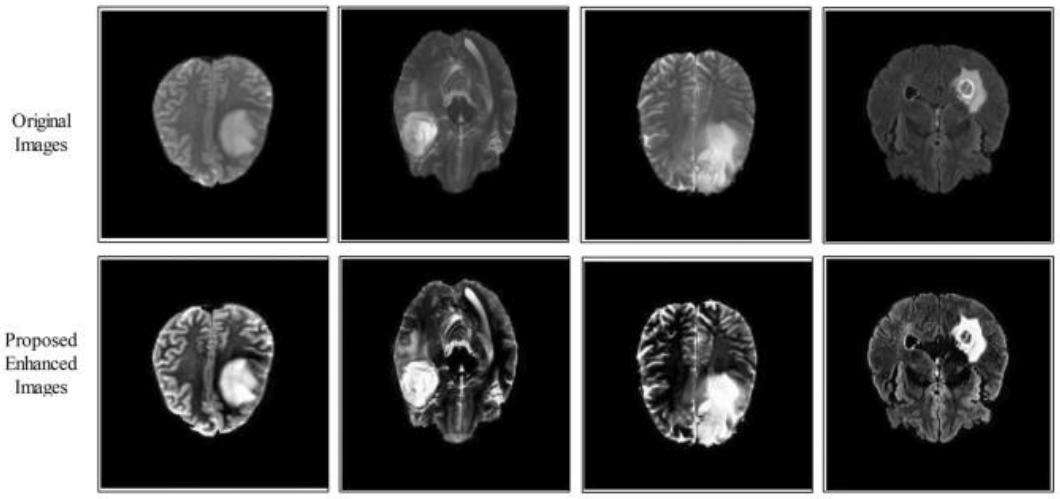

Fig. 4 Proposed contrast enhancement results using ANN-RF-SVM Classifiers

There areseven levels to the ANN model utilized here. The initial flatten layer flattens the 256x256x3 photos into a 1D array.Following a single sparse layer, there are five dense layers with activation functions of relu and neuron counts of 128, 256, 512, 256, and 128 single neuron represents the two classes in the last dense layer whose activation function is sigmoid, which acts as the output layer.These five layers serve as the hidden layers, while the final dense layer with a sigmoid activation function serves as the output layer, each class being represented by a single neuron.

1. Setup of Weights and Bias

2. Procedural feedback loop

3. Errors that are repeated in reverse

4. Improvements to priors and weights

I. Setup of Weights and Bias

Step 1: Start with small, random numbers close to zero as the weights.

Step 2: Perform steps 3–10 so long as the stop condition is not met.

Step 3: Repeat steps 4-9 for each training pair. Inputs that are fed forward

Step 4: The ith input xi is obtained and passed on to the hidden layers above.

Step 5: Sum of the weighted inputs is computed by the hidden unit as

$RZinj = FWoj + \Sigma rxirwij$

Making use of the Activation function

$RZj = f(RZinj)$

To the output layer we send this value.

Step 6: A weighted sum of input units is the output unit.

$Fyink = FVoj + \Sigma RZjFVjk$

Putting in Practise the Activation Function

$FYk = f(Fyink)$

III. The Error Backpropagation Process

Step 7: $\delta sk = (tsk - fYk)f(fyink)$

Step 8: $\delta inj = \Sigma \delta jFVjk$

IV. Revised weighting and biassing

Step 8: Weight correction is Δrwij = αδrkZj

bias Correction is Δfwoj = αδfk

Ratio and Proportionality Corrections

Step 9: kept going:

The New Load

ANNWij(imagenew) = ANNWij(imageold) + Δrwij

NNVjk(imagenew) = NNVjk(imageold) + ΔFVjk

New bias is

ANNWoj(imagenew) = ANNWoj(imageold) + Δrwoj

NNVok(imagenew) = NNVok(imageold) + ΔFVok

Step 10: Verify Termination of Action

5. RESULT AND DISCUSSION

For this study, we consult the BRATS-2015 reference data set. The experimentMR brain pictures used in the proposed system include 126 tumored images and 174 normal images. The data set is randomly split into three parts: 60% for training, 20% for verification, and the remaining 20% for testing. Differentiating a high-den and a low-den MR brain images is possible. Model creation and testing occurred in the MATLAB 2020 development environment on a machine with an Intel i7 processor and 8 GB of RAM.

This research makes use of 250 magnetic resonance scans of the brain from the BRATS database. Sixteen MR brain slices (coronal, axial, and sagittal) were obtained for this study. T1w, T2w, and FLAIR modalities are all derived from the retrieved MR brain slices. Brain slices obtained from MRI scans are utilised for random exercises in learning, testing, and verification.

The outcome of a simulation run using three test MR brain pictures and the proposed ANN-SVM-RF technique. The input MR brain picture that was used to train the proposed ANN-SVM-RF model. Anisotropic diffusion is used as a filter on the initial magnetic resonance (MR) image. Figure 5B shows an MR image of the brain after smoothing, with the edge information still intact. Therefore, it offers a method to enhance accuracy when segmenting tumour regions. After that, the image after filtering is sent on to the ANN-SVM-RF method. The retrieved features are used by the ANN-SVM-RF model to reliably label the MR brain picture as abnormal or normal.

Using a bounding box and an ANN-SVM-RF model, we were able to pinpoint the area of the filtered MR brain image that contained the tumor. The MR brain picture is then coloured green to identify the regions where the tumor was excised. The grayscale morphological operation is then used to precisely segment the tumor regions. Filtering followed by the ANN-SVM-RF method produces excellent results for tumor segmentation and classification. Using grayscale morphological techniques, the discovered tumor regions in the MR brain picture are properly segmented.

Table 1 ANN-SVM-RF model Feature Selection Algorithm

Methods %	Sensitivity	Specificity	Accuracy
SWT-GCNN	74	74	71.5
	77	78	73.5
	78	75.7	74.2
	78.6	79.8	75.7
	81.8	82	75.6
	87.23	94.81	95.19
Patch-based CNN	82.6	83.3	84.7
	86.3	87.6	83.4
	91.3	92.5	93.2
	95	96	94.5

	96	96.2	93.6
	91.22	98.39	95.01
Dual force CNN	98.4	97.7	95.3
	93.2	94.6	93.2
	93.3	95.2	94.4
	94.1	95.5	95.2
	95.3	96.4	96.6
Proposed ANN-RF-SVM	96.01	97.41	98.22

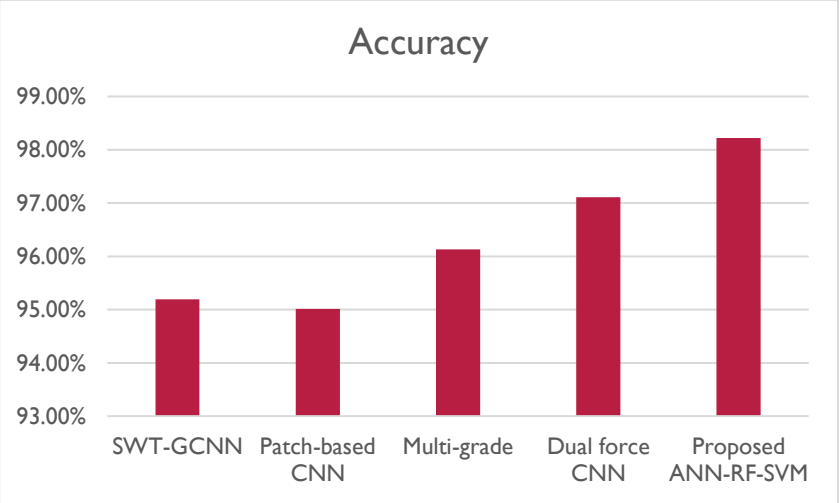

Fig. 5 Enhancement classification accuracy results using ANN-RF-SVM Classifiers

As can be shown in Figure 2, SWT-GCNN outperforms Patch-based CNN, Multi-grade, Dual force CNN, and the proposed ANN-RF-SVM in terms of classification accuracy (4.09%), specificity (2.02%), and sensitivity (2.24%).

As can be seen in Figure 4, SWT-GCNN outperforms Patch-based CNN, Multi-grade, Dual force CNN, and the proposed ANN-RF-SVM in terms of classification accuracy by 5.09%, 3.02%, and 1.24%, respectively.

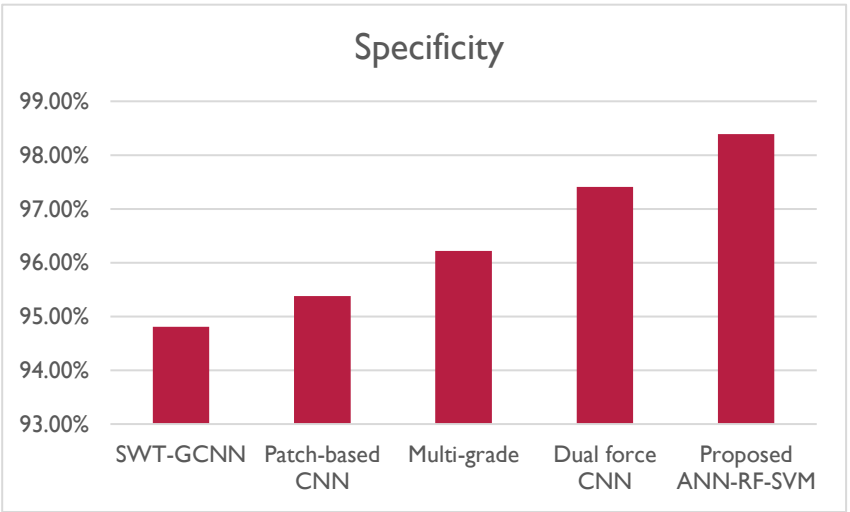

Fig. 6 Enhancement classification specificity results using ANN-RF-SVM Classifiers

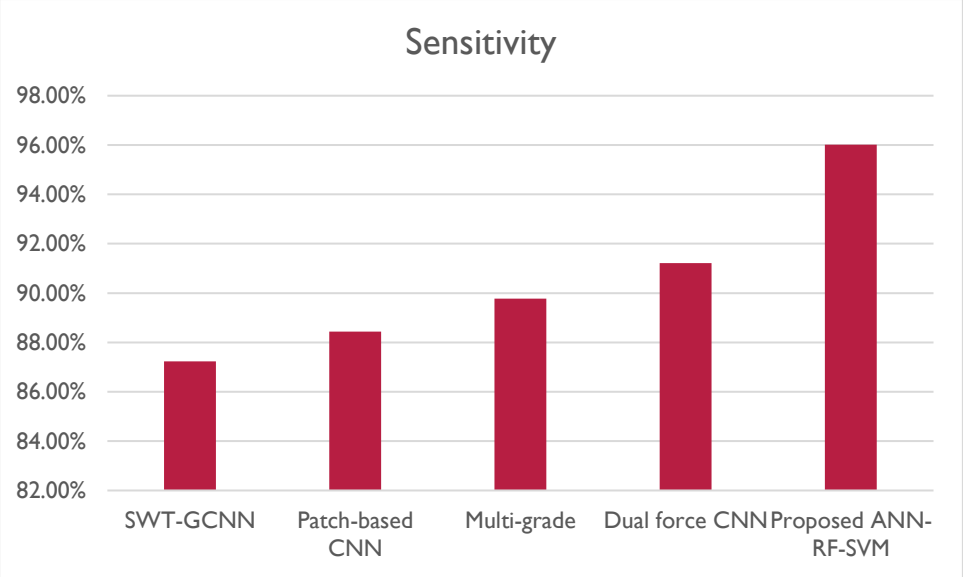

Fig. 7Enhancement classification senitivity results using ANN-RF-SVM Classifiers

Table 2 ANN-SVM-RF model tumor detection Feature Selection Algorithm

GAR %	True Positive Rate - Abnormal	True Positive Rate – MCI	True Positive Rate –Normal
SWT-GCNN	68.5	68	66.5
	72	72.5	68
	72.5	72.5	68
	73.5	74.5	69
	76	76.5	70
	77	75.5	71.5
Patch-based CNN	76.5	75.5	79.5
	81	82	77.5
	85.5	85	86
	88	91	89
	93	90.5	88
	92	90.5	90
Dual force CNN	92	92.5	89.5
	92	91.5	88.5
	94	92	88
	93	91	88
	92	92.5	89.5
Proposed ANN-RF-SVM	92.78	90.92	89.11

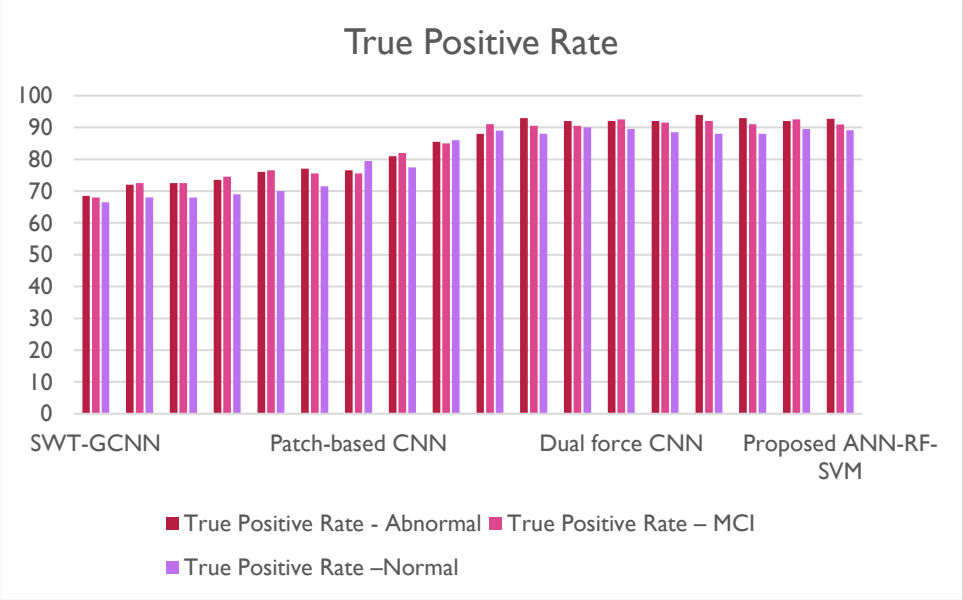

Fig. 8 Enhancement classification True Positive Rate results using ANN-RF-SVM Classifiers

The proposed ANN-RF-SVM improved the true positive rate for Dual force CNN from 5% to 6.25%. See Figure 3 for details. ANN-RF-SVM achieved 4.51%, while Patch-based CNN achieved 0.98%. Compared to Multi-grade (14.74%), SWT-GCNN (10.84%), and Patch-based CNN (3.7%), the ANN-RF-SVM's true positive rate for MCI is greater. True positive rates for tumour detection range from 6.25 percent for SWT-GCNN to 6.45 percent for patch-based CNN and 6.44 percent for Dual force CNN. The average true positive rate was 7.16% for Patch-based CNN, 5.77% for Multi-grade CNN, and 5.09% for Dual-force CNN and the proposed ANN-RF-SVM.

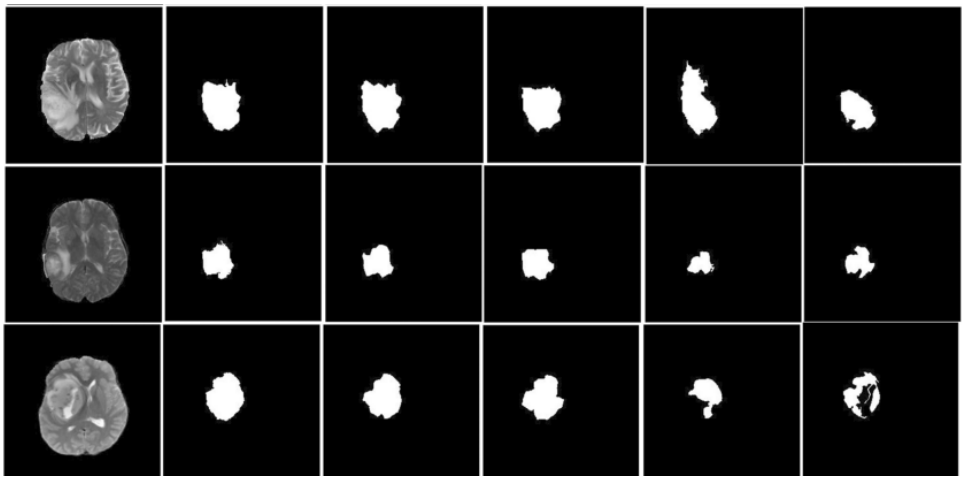

Conclusions and Future Works

Feature engineering gives deep learning an edge over other machine learning methods. This analyses the data to look for related qualities and includes them to speed up the learning process. utilise input spatial consistency. Training and testing come after the initial image processing step of selecting and extracting features. Improved accuracy in detecting and segmenting brain tumors in MR images is demonstrated here using an anisotropic diffusion-filtered ANN-RF-SVM technique. Using the proposed ANN-RF-SVM method, we were able to extract and classify features from the processed MR brain pictures. The performance of the suggested approach is compared to that of existing methods using a sensitivity, specificity, and accuracy metre. The evaluation outcomes showed that the suggested ANN-RF-SVM approach provides significantly more significant outcomes than the current approaches. Medical image processing will benefit greatly from the suggested ANN-RF-SVM method because of how well it can detect and isolate tumours. The proposed method, however, requires a substantial quantity of information and settings used to refine a model and produce reliable results. The suggested system relies on the qualities of the target image, which necessitates subjective empirical parameter adjustment. An optimisation algorithm will be used to accurately choose the parameter value in a future iteration of the suggested method.

To further improve brain tumour classification, A higher number of layers will be added to the proposed system, and data augmentation techniques will be integrated.

Data Availability

Data availability Author Confirms the data availability which is related to this manuscript in case the requirements for research targets.

Declarations

Conflict of interest Authors declare wish to confirm that there are no known conflicts of interest associated with this publication and there has been no significant financial support for this work that could have influenced its outcome.

REFERENCES

[1] Sert E, Ozyurt F, Dogantekin A. A new approach for brain tumor diagnosis system: single image super resolution based

[2] maximum fuzzy entropy segmentation and convolutional neural network. Med Hypotheses. 2019;133:109413. doi:10.1016/j.mehy.2019.109413

[3] Ozyurt F, Sert E, Avci E, Dogantekin E. Brain tumor detection based on convolutional neural network with neutrosophic expert maximum fuzzy sure entropy. Measurement. 2019;147: 106830. doi:10.1016/j.measurement.2019.07.058

[4] Mittal M, Goyal M, Kaur S, Kaur I, Verma A, Hemanth J. Deep learning based enhanced tumor segmentation approach for MR brain images. Appl Soft Comput. 2019;78:346-354. doi: 10.1016/j.asoc.2019.02.036

[5] Hussain S, Anwar M, Majid M. Segmentation of glioma tumors in brain using deep convolutional neural network. Neurocomputing. 2018;282:248-261. doi:10.1016/j.neucom.2017.12.032

[6] Nema S, Dudhane A, Murala S, Naidu S. RescueNet: an unpaired GAN for brain tumor segmentation. Biomed Signal Process Control. 2020;55:101641. doi:10.1016/j.bspc.2019.101641

[7] Khan H, Shah M, Shah A, Islam U, Rodrigues J. Cascading handcrafted features and Convolutional Neural Network for IoT-enabled brain tumor segmentation. Comput Commun. 2020;153:196-207. doi:10.1016/j.comcom.2020.01.013

[8] Chang J, Zhang L, Gu N, et al. A mix-pooling CNN architecture with FCRF for brain tumor segmentation. J Vis Commun Image Represent. 2019;58:316-322. doi:10.1016/j.jvcir.2018. 11.047

[9] Sajjad M, Khan S, Muhammad K, Wu W, Ullah A, Baik W. Multi-grade brain tumor classification using deep CNN with extensive data augmentation. J Comput Sci. 2019;30:174-182. doi:10.1016/j.jocs.2018.12.003

[10] Saravanan, T., Saravanakumar, S., Rathinam, G. O. P. A. L., Narayanan, M., Poongothai, T., Patra, P. S. K., & Sengan, S. U. D. H. A. K. A. R. (2022). Malicious attack alleviation using improved time-based dimensional traffic pattern generation in uwsn. *Journal of Theoretical and Applied Information Technology*, *100*(3), 682-689.

[11] Sisik F, Sert E. Brain tumor segmentation approach based on the extreme learning machine and significantly fast and robust fuzzy C-means clustering algorithms running on Raspberry Pi hardware. Med Hypotheses. 2020;136:109507. doi:10.1016/j.mehy.2019.109507

[12] Chen S, Ding C, Liu M. Dual-force convolutional neural networks for accurate brain tumor segmentation. Pattern Recogn.2019;88:90-100. doi:10.1016/j.patcog.2018.11.009

[13] Mlynarski P, Delingette H, Criminisi A, Ayache N. 3D convolutional neural networks for tumor segmentation using longrange 2D context. Comput Med Imaging Graph. 2019;73:60-72.doi:10.1016/j.compmedimag.2019.02.001

[14] Palma A, Cappabianco A, Jaime S, Miranda P. Anisotropic diffusion filtering operation and limitations-magnetic resonance imaging evaluation. IFAC Proc Vol. 2014;47(3):3887-3892. doi:10.3182/20140824-6-ZA-1003.02347

[15] Niu X, Suen C. A novel hybrid CNN–SVM classifier for recognizing handwritten digits. Pattern Recogn. 2012;45(4):1318-1325. doi:10.1016/j.patcog.2011.09.021

[16] Selvapandian A, Manivannan K. Performance analysis of meningioma brain tumor classifications based on gradient boosting classifier. Int J Imaging Syst Technol. 2018;28(4):295- 301. doi:10.1002/ima.22288

[17] Menze BH, Jakab A, Bauer S, et al. The multimodal brain tumor image segmentation benchmark (BRATS). IEEE Trans Med Imaging. 2015;34(10):1993-2024. doi:10.1109/TMI.2014.2377694

[18] Saravanakumar, S. (2020). Certain analysis of authentic user behavioral and opinion pattern mining using classification techniques. *Solid State Technology*, *63*(6), 9220-9234.

[19] Othman, S. B., Almalki, F. A., &Sakli, H. (2022). Internet of things in the healthcare applications: overview of security and privacy issues. Intelligent Healthcare, 195-213.

[20] Ang, K. L. M., Seng, J. K. P., &Ngharamike, E. (2022). Towards crowdsourcing internet of things (crowd-iot): Architectures, security and applications. Future Internet, 14(2), 49.

[21] Saravanan, T., &Saravanakumar, S. (2021, December). Privacy Preserving using Enhanced Shadow Honeypot technique for Data Retrieval in Cloud Computing. In 2021 3rd International Conference on Advances in Computing, Communication Control and Networking (ICAC3N) (pp. 1151-1154). IEEE.

[22] Behera, N. K. S., Behera, T. K., Nappi, M., Bakshi, S., & Sa, P. K. (2021). Futuristic person re-identification over internet of biometrics things (IoBT): Technical potential versus practical reality. Pattern Recognition Letters, 151, 163-171.

[23] Qadri, Y. A., Nauman, A., Zikria, Y. B., Vasilakos, A. V., & Kim, S. W. (2020). The future of healthcare internet of things: a survey of emerging technologies. IEEE Communications Surveys & Tutorials, 22(2), 1121-1167.

[24] Saravanakumar, S., & Saravanan, T. (2023). Secure personal authentication in fog devices via multimodal rank-level fusion. *Concurrency and Computation: Practice and Experience*, *35*(10), e7673.

[25] Thangavel, S., & Selvaraj, S. (2023). Machine Learning Model and Cuckoo Search in a modular system to identify Alzheimer's disease from MRI scan images. *Computer Methods in Biomechanics and Biomedical Engineering: Imaging & Visualization*, *11*(5), 1753-1761.